

Rao-Blackwellized particle smoothers for conditionally linear Gaussian models*

Fredrik Lindsten, Pete Bunch, Simo Särkkä,
Thomas B. Schön, and Simon J. Godsill

23 May 2015

Abstract

Sequential Monte Carlo (SMC) methods, such as the particle filter, are by now one of the standard computational techniques for addressing the filtering problem in general state-space models. However, many applications require post-processing of data offline. In such scenarios the smoothing problem—in which all the available data is used to compute state estimates—is of central interest. We consider the smoothing problem for a class of *conditionally linear Gaussian* models. We present a forward-backward-type Rao-Blackwellized particle smoother (RBPS) that is able to exploit the tractable substructure present in these models. Akin to the well known Rao-Blackwellized particle filter, the proposed RBPS marginalizes out a conditionally tractable subset of state variables, effectively making use of SMC only for the “intractable part” of the model. Compared to existing RBPS, two key features of the proposed method are: *(i)* it does not require structural approximations of the model, and *(ii)* the aforementioned marginalization is done both in the forward direction and in the backward direction.

1 Introduction

State-space models (SSMs) comprise one of the most important model classes in statistical signal processing, automatic control, econometrics, and related areas. A general discrete-time SSM is given by

$$x_{t+1} \sim p(x_{t+1} | x_t), \quad (1a)$$

$$y_t \sim p(y_t | x_t), \quad (1b)$$

where $x_t \in \mathbb{R}^{n_x}$ is the latent state process and $y_t \in \mathbb{R}^{n_y}$ is the observed measurement process (we use the common convention that p denotes an arbitrary

*Supported by the projects *Learning of complex dynamical systems* (Contract number: 637-2014-466) and *Probabilistic modeling of dynamical systems* (Contract number: 621-2013-5524), both funded by the Swedish Research Council, and the project *Bayesian Tracking and Reasoning over Time* (Reference: EP/K020153/1), funded by the EPSRC.

probability density function (PDF) induced by the model (1), which is identified by its arguments). When the model is linear and Gaussian the filtering and smoothing problems can be solved optimally by using methods such as the Kalman filter and the Rauch-Tung-Striebel smoother, respectively (see, e.g., [18]). When going beyond the linear Gaussian case, however, no analytical solution for the optimal state inference problem is available, which calls for approximate computational methods.

Many popular deterministic methods are based on Gaussian approximations, for instance through linearization and related techniques. An alternative approach, for which the accuracy of the approximation is limited basically only by the computational budget, is to use Monte Carlo methods. Among these, sequential Monte Carlo (SMC) methods such as particle filters (PF) and particle smoothers (PS) play a prominent role (see, e.g., [10, 15]).

While SMC can be applied directly to the general model (1), it has been recognized that, in many cases, there is a tractable substructure available in the model. This structure can then be exploited to improve the performance of the SMC method. In particular, the Rao-Blackwellized PF (RBPF) [29, 7] has been found to be very useful for addressing the filtering problem in *conditionally linear Gaussian* (CLG) SSMS (see Section 2). As pointed out in [6], CLG models have found an “exceptionally broad range of applications”.

However, many of the applications, as well as system identification, of SSMS rely on batch analysis of data. The central object of interest is then the smoothing distribution, that is, the distribution of the system state(s) conditionally on all the observed data. While there exist many SMC-based smoothers (see e.g., [23] and the references therein) variance reduction by Rao-Blackwellization has not been as well explored for smoothing as for filtering.

In this paper, we present a Rao-Blackwellized PS (RBPS) for general CLG models. The proposed method is based on the forward filter/backward simulator (FFBS) [13]. Contrary to the related forward-backward-type RBPS used by [19], the proposed method does not require any structural approximations of the model. Another key feature of the proposed method is that it employs Rao-Blackwellization both in the forward and backward directions, as opposed to [11] who sample the full system state in the backward direction. The use of Rao-Blackwellization also in the backward direction is necessary for the smoother to be truly Rao-Blackwellized. An alternative RBPS, specifically targeting the marginal smoothing distribution, which is based on the generalized two-filter formula is presented in [4].

This contribution builds upon two previous conference publications, [27] and [22], where we studied two specific model classes, hierarchical models and mixed linear/nonlinear models, respectively (see the next section for definitions). Furthermore, independently of [27], Whiteley et al. [32] have derived essentially the same RBPS for hierarchical models as we present here, although they study explicitly the special case of jump Markov systems. The present work goes beyond [27, 22] on several accounts. First, the techniques used for the derivations and, as an effect, details of the algorithmic specifications in these two proceedings differ substantially. Here, we harmonise the derivation and provide a general al-

gorithm which is applicable to both types of CLG models under study. We also improve the previous results by extending the method to more general models. Specifically, we allow for correlation between the process noises entering the conditionally linear and the nonlinear parts of the model, and rank-deficient process noise covariances in the conditionally linear parts. This comprises an important class of models in practical applications [16]. Finally, we provide several extensions to the main method (Section 5) that we view as a key part of the proposed methodology.

For a vector μ and a positive semidefinite matrix $\Omega \succeq 0$, we write $\|\mu\|_{\Omega}^2 \triangleq \mu^{\top} \Omega \mu$. We write $|A|$ for matrix determinant and $\mathcal{N}(\mu, \Sigma)$ and $\mathcal{N}(x; \mu, \Sigma)$ for the Gaussian distribution and PDF, respectively.

2 Conditionally linear Gaussian models

Let the system state be partitioned into two parts: $x_t = (u_t, z_t)$, where $u_t \in \mathbb{R}^{n_u}$ is referred to as the *nonlinear state* and $z_t \in \mathbb{R}^{n_z}$ is referred to as the *linear state*. The SSM (1) is said to be CLG if the conditional process $\{z_t, y_t \mid u_{1:t}\}_{t \geq 1}$ follows a time-inhomogeneous linear Gaussian SSM. For concreteness, we will study two specific classes of CLG models, which are of particular practical interest. However, by combining these two model classes the proposed method can straightforwardly be generalized to other CLG models.

Model 1 (Hierarchical CLG model) *A hierarchical CLG model is given by,*

$$u_{t+1} \sim p(u_{t+1} \mid u_t), \quad (2a)$$

$$z_{t+1} = f(u_{t+1}) + A(u_{t+1})z_t + F(u_{t+1})v_t, \quad (2b)$$

$$y_t = h(u_t) + C(u_t)z_t + e_t, \quad (2c)$$

with process noise $v_t \sim \mathcal{N}(0, I_{n_v})$ and measurement noise $e_t \sim \mathcal{N}(0, R(u_t))$, respectively, where $R(u_t)$ is a positive definite matrix for any $u_t \in \mathbb{R}^{n_u}$.

Model 1 can be seen as a generalization of a *jump Markov system*, in which the “jump” or “mode” variable u_t is allowed to be continuous. However, the hierarchical structure of Model 1 can sometimes be limiting. We will therefore study also the following model class.

Model 2 (Mixed linear/nonlinear model) *A mixed linear/nonlinear CLG model is given by,*

$$\begin{bmatrix} u_{t+1} \\ z_{t+1} \end{bmatrix} = \begin{bmatrix} g(u_t) \\ f(u_t) \end{bmatrix} + \begin{bmatrix} B(u_t) \\ A(u_t) \end{bmatrix} z_t + \begin{bmatrix} G(u_t) \\ F(u_t) \end{bmatrix} v_t, \quad (3a)$$

$$y_t = h(u_t) + C(u_t)z_t + e_t, \quad (3b)$$

with process noise $v_t \sim \mathcal{N}(0, I_{n_v})$ and measurement noise $e_t \sim \mathcal{N}(0, R(u_t))$, respectively, where $Q(u_t) \triangleq G(u_t)G(u_t)^{\top}$ and $R(u_t)$ are assumed to be positive definite matrices for any $u_t \in \mathbb{R}^{n_u}$.

Note that Model 2 allows for a cross-dependence in the dynamics of the two state-components, that is u_{t+1} depends explicitly on z_t and *vice versa*. Mixed linear/nonlinear models arise, for instance, when the observations depend nonlinearly on a subset of the states in a system with linear dynamics. See [16] for several examples from target tracking where this model is used.

Remark 1 *We do not assume that $F(u_t)F(u_t)^\top$ is full rank, that is, it is only the part of the process noise that enters on the nonlinear state u_t that is assumed to be non-degenerate. Note also that the model (3a) readily allows for correlation between the components of the process noise entering on the nonlinear state and on the linear state, respectively.*

It is worth to emphasize that Model 1 is *not* a special case of Model 2, since $p(u_{t+1} | u_t)$ may be non-Gaussian in (2a). Nevertheless, Model 1 is simpler than Model 2 in many respects. Indeed, one reason for why we study both model classes in parallel is to more clearly convey the idea of the derivation. This is possible since we can start by looking at the (simpler) hierarchical CLG model, before generalizing the expressions to the (more involved) mixed linear/nonlinear model.

3 Background

3.1 Particle filtering and smoothing

Consider first the general SSM (1). A PF is an SMC algorithm used to approximate the intractable filtering density $p(x_t | y_{1:t})$ (see e.g. [10, 15]). Rather than targeting the sequence of filtering densities directly, however, the PF targets the sequence of joint smoothing densities $p(x_{1:t} | y_{1:t})$ for $t = 1, 2, \dots$. This is done by representing $p(x_{1:t} | y_{1:t})$ with a set of weighted particles $\{x_{1:t}^i, w_t^i\}_{i=1}^N$, each of which is a state trajectory $x_{1:t}$. These particles define the point-mass approximation,

$$\hat{p}^N(x_{1:t} | y_{1:t}) \triangleq \sum_{i=1}^N w_t^i \delta_{x_{1:t}^i}(x_{1:t}), \quad (4)$$

where δ_x denotes a Dirac distribution at point x . In the simplest particle filter, the t -th set of particles are formed by sampling $x_{1:t-1}$ from the previous distribution (resampling) and then x_t from an importance distribution $q(x_t | x_{1:t-1}, y_t)$. A weight is assigned to each particle to account for the discrepancy between the proposal and the target density. The importance weight is given by the ratio of target and proposal densities, which simplifies to,

$$w_t(x_{1:t}) \propto \frac{p(y_t | x_t)p(x_t | x_{t-1})}{q(x_t | x_{1:t-1}, y_t)}. \quad (5)$$

Note that an approximation to $p(x_t | y_{1:t})$ is obtained by marginalization of (4), which equates to simply discarding $x_{1:t-1}^i$ for each particle $i = 1, \dots, N$.

The term “smoothing” encompasses a number of related inference problems. Basically, it amounts to computing the posterior PDF of some (past) state variable, given a batch of measurements $y_{1:T}$. Here we focus on the estimation of the complete joint smoothing density, $p(x_{1:T} | y_{1:T})$. Any marginal smoothing density can be computed from the joint smoothing density by marginalization.

In fact, the joint smoothing distribution is approximated at the final step of the particle filter [20]. However, this approximation suffer from the problem of path degeneracy, that is, the number of unique particles decreases rapidly for $t \ll T$ [13, 10]. To mitigate this issue, a diverse set of particles may be generated by sampling state trajectories using the forward filtering/backward simulation (FFBS) algorithm [13]. FFBS exploits a sequential factorization of the joint smoothing density:

$$p(x_{1:T} | y_{1:T}) = p(x_T | y_{1:T}) \prod_{t=1}^{T-1} p(x_t | x_{t+1:T}, y_{1:T}). \quad (6)$$

At time T , a final state \tilde{x}_T is first sampled from the particle filter approximation $\hat{p}^N(x_T | y_{1:T})$. Then, working backward from time T , each subsequent state \tilde{x}_t is sampled (approximately) from the *backward kernel*, $p(x_t | \tilde{x}_{t+1:T}, y_{1:T})$. The resulting trajectory $\tilde{x}_{1:T}$ is then an approximate sample from the joint smoothing distribution.

Using the Markov property, the backward kernel may be expressed as

$$p(x_t | x_{t+1:T}, y_{1:T}) \propto p(x_{t+1} | x_t) p(x_t | y_{1:t}). \quad (7)$$

By using the PF approximation of the filtering distribution, we obtain the following point-mass approximation of the backward kernel:

$$\hat{p}^N(x_t | \tilde{x}_{t+1:T}, y_{1:T}) \triangleq \sum_{i=1}^N \tilde{w}_{t|T}^i \delta_{x_i^i}(x_t), \quad (8)$$

with $\tilde{w}_{t|T}^i \propto w_t^i p(\tilde{x}_{t+1} | x_t^i)$. The FFBS algorithm samples from this approximation in the backward simulation pass.

Typically, we repeat the backward simulation, say, M times. This generates a collection of backward trajectories $\{\tilde{x}_{1:T}^j\}_{j=1}^M$ which define a point-mass approximation of the joint smoothing distribution according to,

$$\tilde{p}^M(x_{1:T} | y_{1:T}) \triangleq \frac{1}{M} \sum_{j=1}^M \delta_{\tilde{x}_{1:T}^j}(x_{1:T}). \quad (9)$$

From this, any marginal or fixed-interval smoothing distribution can be approximated by simply discarding the parts of the backward trajectories which are not of interest.

3.2 Rao-Blackwellized particle filter

We now turn our attention specifically to CLG models, such as Model 1 or Model 2. The structure inherent in these models can be exploited when addressing the filtering problem. This is done in the RBPF, which is based on

the factorization $p(u_{1:t}, z_t | y_{1:t}) = p(z_t | u_{1:t}, y_{1:t})p(u_{1:t} | y_{1:t})$. Since the model is CLG, it holds that

$$p(z_t | u_{1:t}, y_{1:t}) = \mathcal{N}(z_t; \bar{z}_{t|t}(u_{1:t}), P_{t|t}(u_{1:t})), \quad (10)$$

for some mean and covariance functions, $\bar{z}_{t|t}(u_{1:t})$ and $P_{t|t}(u_{1:t})$, respectively. A PF is used to estimate only the nonlinear state marginal density while conditional Kalman filters, one for each particle, are used to compute the moments for the linear state in (10). The resulting RBPF approximation is given by

$$\hat{p}^N(u_{1:t}, z_t | y_{1:t}) = \sum_{i=1}^N w_t^i \mathcal{N}(z_t; \bar{z}_{t|t}^i, P_{t|t}^i) \delta_{u_{1:t}^i}(u_{1:t}),$$

where $\bar{z}_{t|t}^i = \bar{z}_{t|t}(u_{1:t}^i)$ and $P_{t|t}^i = P_{t|t}(u_{1:t}^i)$. The particle weights are given by the ratio of $p(y_t, u_t | u_{1:t-1}, y_{1:t-1})$ and the importance density. See [7] for details on the implementation for the hierarchical CLG model and [29] for the mixed linear/nonlinear model. The reduced dimensionality of the particle approximation results in a reduction in variance of associated estimators [24, 8].

For numerical stability, it is recommended to implement the conditional Kalman filters on square-root form. That is, we propagate, e.g., the Cholesky factor $\Gamma_{t|t}(u_{1:t})$ of the conditional covariance matrix, rather than the covariance matrix itself, where $\Gamma_{t|t}(u_{1:t})$ is such that

$$P_{t|t}(u_{1:t}) = \Gamma_{t|t}(u_{1:t})\Gamma_{t|t}(u_{1:t})^\top. \quad (11)$$

See Section 5.3.

4 Rao-Blackwellized particle smoothing

We now turn to the derivation of the new RBPS. The method is an FFBS which uses the RBPF as a forward filter. The novelty lies in the construction of a backward simulator which samples only the nonlinear state in the backward pass. Difficulty arises because marginally (and conditionally on the observations) the nonlinear state process is non-Markovian. Practically, this means that the backward kernel cannot be expressed in a simple way, as in (7). We address this difficulty by deriving a backward recursion for a set of sufficient statistics for the backward kernel. This backward recursion is reminiscent of the backward filter in the two-filter smoothing formula for a linear Gaussian SSM (see e.g., [18, Chapter 10]).

The basic idea is presented in Section 4.1, together with the statement of a general algorithm which samples state trajectories for the nonlinear states. We then consider the two specific model classes, the hierarchical CLG model and the mixed linear/nonlinear model, in Section 4.2 and Section 4.3, respectively. In Section 4.4 we discuss how to compute the smoothing distribution for the linear states.

4.1 Rao-Blackwellized backward simulation

We wish to derive a backward simulator for the nonlinear process $\{u_t\}$. That is, the target density is $p(u_{1:T} | y_{1:T})$. However, when marginalizing the linear states $\{z_t\}$, we introduce a dependence in the measurement likelihood on the complete history $u_{1:t}$. As a consequence, we must sample complete trajectories produced by the RBPF when simulating the nonlinear backward trajectories; see [23, Chapter 4] for a general treatment of backward simulation in the non-Markovian setting. To solidify the idea, note that the target density can be expressed as

$$p(u_{1:T} | y_{1:T}) = p(u_{1:t} | u_{t+1:T}, y_{1:T})p(u_{t+1:T} | y_{1:T}). \quad (12)$$

Assume that we have run a backward simulator from time T down to time $t+1$. Hence, we have generated a partial, nonlinear backward trajectory $\tilde{u}_{t+1:T}$, which is an approximate sample from $p(u_{t+1:T} | y_{1:T})$. To extend this trajectory to time t , we draw one of the RBPF particles $\{u_{1:t}^i\}_{i=1}^N$ (with probabilities computed below). We then set $\tilde{u}_{t:T} = \{u_t^i, \tilde{u}_{t+1:T}\}$ and discard $u_{1:t-1}^i$. This procedure is then repeated for each time $t = T-1, \dots, 1$, resulting in a complete backward trajectory $\tilde{u}_{1:T}$.

To compute the backward sampling probabilities, we note that the first factor in (12) can be expressed as,

$$p(u_{1:t} | u_{t+1:T}, y_{1:T}) \propto p(y_{t+1:T}, u_{t+1:T} | u_{1:t}, y_{1:t})p(u_{1:t} | y_{1:t}). \quad (13)$$

The second factor in this expression can be approximated by the forward RBPF, analogously to a standard FFBS. Similarly to (8), this results in a point-mass approximation of the backward kernel, given by

$$\hat{p}^N(u_{1:t} | \tilde{u}_{t+1:T}, y_{1:T}) = \sum_{i=1}^N \tilde{w}_{t|T}^i \delta_{u_{1:t}^i}(u_{1:t}), \quad (14)$$

with

$$\tilde{w}_{t|T}^i \propto w_t^i p(y_{t+1:T}, \tilde{u}_{t+1:T} | u_{1:t}^i, y_{1:t}). \quad (15)$$

We thus employ the following backward simulation strategy to sample $\tilde{u}_{1:T} \stackrel{\text{approx.}}{\sim} p(u_{1:T} | y_{1:T})$:

1. Run a forward RBPF for times $t = 1, \dots, T$.
2. Sample \tilde{u}_T with with $\mathbb{P}(\tilde{u}_T = u_T^i) = w_T^i$.
3. For $t = T-1$ to 1:
 - (a) Sample \tilde{u}_t with $\mathbb{P}(\tilde{u}_t = u_t^i) = \tilde{w}_{t|T}^i$.
 - (b) Set $\tilde{u}_{t:T} = \{\tilde{u}_t, \tilde{u}_{t+1:T}\}$.

Note that Step 3a) effectively means that we simulate $u_{1:t}^i$ from the point-mass approximation of the backward kernel (14), discard $u_{1:t-1}^i$, and set $\tilde{u}_t = u_t^i$. More detailed pseudo-code is given in Algorithm 1 below.

It remains to find an expression (up to proportionality) for the predictive PDF in (15), in order to compute the backward sampling weights. In fact, since the model is CLG, this PDF can be computed straightforwardly by running a conditional Kalman filter from time t up to T . However, using such an approach to calculate the weights at time t would require N separate Kalman filters to run over $T - t$ time steps, resulting in a total computational complexity scaling quadratically with T . To avoid this, we seek a more efficient computation of the weights (15). This is accomplished by propagating a set of sufficient statistics backward in time, as the trajectory $\tilde{u}_{1:T}$ is generated. Specifically, these statistics are computed by running a conditional backward information filter for z_t , conditionally on $\tilde{u}_{t:T}$, $t = T, T - 1, \dots, 1$. The idea stems from [12], who use the same approach for Markov chain Monte Carlo sampling in jump Markov systems.

To see how this can be done, note that the predictive PDF in (15) can be expressed as

$$\begin{aligned} p(y_{t+1:T}, u_{t+1:T} \mid u_{1:t}, y_{1:t}) \\ = \int p(y_{t+1:T}, u_{t+1:T} \mid z_t, u_t) p(z_t \mid u_{1:t}, y_{1:t}) dz_t. \end{aligned} \quad (16)$$

This expression is related to the factorization used in the two-filter smoothing formula. The second factor of the integrand is the conditional forward filtering density. This density, computed in the forward RBPF, is given by (10). Similarly, we can view the first factor of the integrand as the density targeted by a conditional backward filter, akin to the one used in the two-filter smoothing formula.

Indeed, we will derive a conditional backward information filter for this density, and thereby show that

$$p(y_{t+1:T}, u_{t+1:T} \mid z_t, u_t) \propto Z_t \exp\left(-\frac{1}{2} (z_t^\top \Omega_t z_t - 2\lambda_t^\top z_t)\right), \quad (17)$$

where Z_t , $\Omega_t \succeq 0$ and λ_t depend on u_t , but are independent of z_t , and the proportionality is with respect to (u_t, z_t) .¹ Note that (17) is not a PDF in z_t . Still, it can be instructive to think about the above expression as a Gaussian PDF with information vector λ_t and information matrix Ω_t . We choose to express the backward statistics on information form since, as we shall see later, Ω_t is not necessarily invertible. The interpretation of (17) as a Gaussian PDF for z_t implicitly corresponds to the assumption of a non-informative (flat) prior on z_t . As pointed out above, this interpretation might be useful for understanding the role of the backward statistics, but it does not affect our derivation in any way.

¹By proportionality with respect to some variable x , we mean that the constant hidden in the proportionality sign is independent of this variable.

As an intermediate step of the derivation, we will also show the related identity,

$$p(y_{t:T}, u_{t+1:T} | z_t, u_t) \propto \exp\left(-\frac{1}{2}\left(z_t^\top \widehat{\Omega}_t z_t - 2\widehat{\lambda}_t^\top z_t\right)\right), \quad (18)$$

for some $\widehat{\Omega}_t \succeq 0$ and $\widehat{\lambda}_t$ and where the proportionality is with respect to z_t . Computing (18) given (17) corresponds to the measurement update of the backward information filter (the measurement y_t is taken into account). Similarly, computing (17) given (18), with t replaced by $t - 1$, corresponds to a backward prediction.

Assume for now that (17) holds. To compute the integral (16) we make use of the following lemma. The proof is omitted for brevity, but follows straightforwardly by plugging in the expression for z and carrying out the integration with respect to ξ .

Lemma 1 *Let $\xi \sim \mathcal{N}(0, I)$ and let $z = c + Ax + \Gamma\xi$, for some constant vectors c and x and matrices A and Γ , respectively. Let $\Omega \succeq 0$ and λ be a constant matrix and vector, respectively. Then $\mathbb{E}[\exp(-\frac{1}{2}(z^\top \Omega z - 2\lambda^\top z))]$ = $|M|^{-1/2} \exp(-\frac{1}{2}\gamma)$ with,*

$$\begin{aligned} \gamma = & \|Ax\|_{\Omega - \Omega\Gamma M^{-1}\Gamma^\top\Omega}^2 - 2x^\top A^\top (I - \Omega\Gamma M^{-1}\Gamma^\top) m \\ & + \|c\|_{\Omega}^2 - 2\lambda^\top c - \|\Gamma^\top m\|_{M^{-1}}^2, \end{aligned}$$

where $m = \lambda - \Omega c$ and $M = \Gamma^\top \Omega \Gamma + I$.

From (10) and (11) it follows that if we write

$$z_t = \bar{z}_{t|t} + \Gamma_{t|t}\xi_t, \quad \xi_t \sim \mathcal{N}(0, I), \quad (19)$$

then the distribution of z_t in (19) is $p(z_t | u_{1:t}, y_{1:t})$. In the above, we have dropped the dependence on $u_{1:t}$ for brevity. The integral in (16) can thus be computed by applying Lemma 1 with $c = \bar{z}_{t|t}$, $x = 0$, $\Gamma = \Gamma_{t|t}$, $\Omega = \Omega_t$ and $\lambda = \lambda_t$. It follows that,

$$p(y_{t+1:T}, u_{t+1:T} | u_{1:t}, y_{1:t}) \propto Z_t |\Lambda_t|^{-1/2} \exp(-\frac{1}{2}\eta_t), \quad (20)$$

where the proportionality is with respect to $u_{1:t}$ and with,

$$\eta_t = \|\bar{z}_{t|t}\|_{\Omega_t}^2 - 2\lambda_t^\top \bar{z}_{t|t} - \|\Gamma_{t|t}^\top (\lambda_t - \Omega_t \bar{z}_{t|t})\|_{\Lambda_t^{-1}}^2, \quad (21a)$$

$$\Lambda_t = \Gamma_{t|t}^\top \Omega_t \Gamma_{t|t} + I. \quad (21b)$$

By plugging this result into (15), we obtain an expression for the backward sampling weights. It remains to show the identity (17) and to find the updating equations for the statistics $\{Z_t, \Omega_t, \lambda_t\}$. These recursions will be derived explicitly for the two model classes under study in the consecutive two sections. The resulting Rao-Blackwellized backward simulator is given in Algorithm 1. As for a standard FFBS, the backward simulation is typically repeated M times, to generate a collection of backward trajectories $\{\tilde{u}_{1:T}^j\}_{j=1}^M$ which can be used to approximate $p(u_{1:T} | y_{1:T})$.

Algorithm 1 Rao-Blackwellized backward simulator

1. **Forward filter:** Run an RBPF for time $t = 1, \dots, T$. For each t , store $\{u_t^i, w_t^i, \tilde{z}_{t|t}^i, \Gamma_{t|t}^i\}_{i=1}^N$.
 2. **Initialize:** Draw \tilde{u}_T with $\mathbb{P}(\tilde{u}_T = u_T^i) = w_T^i$. Compute $\hat{\Omega}_T$ and $\hat{\lambda}_T$ according to (23).
 3. **For $t = T - 1$ to 1:**
 - (a) **Backward filter prediction:**

(*Model 1: hierarchical*)

 - Compute $Z_t^i = p(\tilde{u}_{t+1} | u_t^i)$ for $i = 1, \dots, N$.
 - Compute $\{\Omega_t, \lambda_t\}$ according to (25).

(*Model 2: mixed*)

 - Compute $\{Z_t^i, \Omega_t^i, \lambda_t^i\}$ according to (33) for each forward filter particle $i = 1, \dots, N$.
 - (b) For $i = 1, \dots, N$:
 - i. Compute $\{\Lambda_t^i, \eta_t^i\}$ according to (21).
 - ii. Compute $W_t^i = w_t^i Z_t^i |\Lambda_t^i|^{-1/2} \exp(-\frac{1}{2}\eta_t^i)$.
 - (c) Normalize the weights, $\tilde{w}_{t|T}^i = W_t^i / \sum_l W_t^l$.
 - (d) Draw J with $\mathbb{P}(J = i) = \tilde{w}_{t|T}^i$.
 - (e) Set $\tilde{u}_{t:T} = \{u_t^J, \tilde{u}_{t+1:T}\}$.
 - (f) (*Model 2: mixed*) Set $\{\Omega_t, \lambda_t\} = \{\Omega_t^J, \lambda_t^J\}$.
 - (g) **Backward filter measurement update:** Compute $\{\hat{\Omega}_t, \hat{\lambda}_t\}$ according to (27).
-

4.2 Model 1 – Hierarchical CLG model

We now consider Model 1, the hierarchical CLG model, and prove the identities (17) and (18). We also derive explicit updating equations for the statistics $\{Z_t, \Omega_t, \lambda_t\}$ and $\{\widehat{\Omega}_t, \widehat{\lambda}_t\}$, respectively.

Remark 2 *The expressions derived in this section have previously been presented by [32] who, independently from our preliminary work in [27], have derived an RBPS for hierarchical CLG models. Nevertheless, we believe that the present section will be useful in order to make the derivation for the (more involved) mixed linear/nonlinear model in Section 4.3 more accessible.*

For notational simplicity, we write A_t for $A(u_t)$ and similarly for other functions of u_t . To initialize the backward statistics at time T , we note that (2c) can be written as,

$$p(y_T | z_T, u_T) = \mathcal{N}(y_T; h_T + C_T z_T, R_T) \propto \exp\left(-\frac{1}{2} \left(z_T^\top \widehat{\Omega}_T z_T - 2\widehat{\lambda}_T^\top z_T \right)\right), \quad (22)$$

with

$$\widehat{\Omega}_T = C_T^\top R_T^{-1} C_T, \quad (23a)$$

$$\widehat{\lambda}_T = C_T^\top R_T^{-1} (y_T - h_T), \quad (23b)$$

which shows that (18) holds at time $t = T$ (with the convention $u_{T+1:T} = \emptyset$). We continue by using an inductive argument. Hence, assume that (18) holds at some time $t + 1$. To prove (17) we do a backward prediction step. We have, for $t < T$,

$$\begin{aligned} & p(y_{t+1:T}, u_{t+1:T} | z_t, u_t) \\ &= p(u_{t+1} | u_t) \int p(y_{t+1:T}, u_{t+2:T} | z_{t+1}, u_{t+1}) p(z_{t+1} | z_t, u_{t+1}) dz_{t+1}. \end{aligned} \quad (24)$$

Using the induction hypothesis and (2b), the above integral can be computed by applying Lemma 1 with $c = f_{t+1}$, $A = A_{t+1}$, $x = z_t$, $\Gamma = F_{t+1}$, $\Omega = \widehat{\Omega}_{t+1}$ and $\lambda = \widehat{\lambda}_{t+1}$. It follows that (24) coincides with (17), with

$$Z_t = p(u_{t+1} | u_t), \quad (25a)$$

$$\Omega_t = A_{t+1}^\top \left(I - \widehat{\Omega}_{t+1} F_{t+1} M_{t+1}^{-1} F_{t+1}^\top \right) \widehat{\Omega}_{t+1} A_{t+1}, \quad (25b)$$

$$\lambda_t = A_{t+1}^\top \left(I - \widehat{\Omega}_{t+1} F_{t+1} M_{t+1}^{-1} F_{t+1}^\top \right) m_{t+1}, \quad (25c)$$

where we have defined the quantities $m_{t+1} \triangleq \widehat{\lambda}_{t+1} - \widehat{\Omega}_{t+1} f_{t+1}$ and $M_{t+1} \triangleq F_{t+1}^\top \widehat{\Omega}_{t+1} F_{t+1} + I$. Note that the above statistics depend on u_t only through the factor $p(u_{t+1} | u_t)$ in (25a). This is important from an implementation point

of view, since it implies that we do not need to make the backward prediction for each forward filter particle; see Algorithm 1.

Next, to prove (18) for $t < T$, we assume that (17) holds at time t . We have,

$$p(y_{t:T}, u_{t+1:T} | z_t, u_t) = p(y_t | z_t, u_t) p(y_{t+1:T}, u_{t+1:T} | z_t, u_t). \quad (26)$$

The first factor is given by (2c), analogously to (23), and the second factor is given by (17). By collecting terms from the two factors, we see that (26) coincides with (18), where

$$\widehat{\Omega}_t = \Omega_t + C_t^\top R_t^{-1} C_t, \quad (27a)$$

$$\widehat{\lambda}_t = \lambda_t + C_t^\top R_t^{-1} (y_t - h_t). \quad (27b)$$

As pointed out above, this correspond to the backward measurement update. Since we are working with the information form of the backward filter, the measurement update simply corresponds to the addition of a term to the information vector and the information matrix, respectively.

4.3 Model 2 – Mixed linear/nonlinear CLG model

We now turn to the mixed linear/nonlinear model (3) and prove the identities (17) and (18) for this class of systems. First, note that the measurement equations are identical for the models (2) and (3). Consequently, the initialization (23) and the backward measurement update (27) hold for the mixed linear/nonlinear model as well. We will thus focus on the backward prediction step.

Similarly to (24) we factorize the backward prediction density according to,

$$\begin{aligned} & p(y_{t+1:T}, u_{t+1:T} | z_t, u_t) \\ &= p(u_{t+1} | u_t, z_t) \int p(y_{t+1:T}, u_{t+2:T} | z_{t+1}, u_{t+1}) p(z_{t+1} | z_t, u_t, u_{t+1}) dz_{t+1}. \end{aligned} \quad (28)$$

Note that the first factor now depends on z_t . From (3a), we can express this density as,

$$\begin{aligned} p(u_{t+1} | z_t, u_t) &= \mathcal{N}(u_{t+1}; g_t + B_t z_t, Q_t) \\ &\propto |Q_t|^{-1/2} \exp\left(-\frac{1}{2} \left(\|u_{t+1} - g_t\|_{Q_t^{-1}}^2\right)\right) \\ &\quad \times \exp\left(-\frac{1}{2} \left(\|B_t z_t\|_{Q_t^{-1}}^2 - 2z_t^\top B_t^\top Q_t^{-1} (u_{t+1} - g_t)\right)\right). \end{aligned} \quad (29)$$

Next, we address the integral in (28). Since the process noise v_t enters the expressions for both u_{t+1} and z_{t+1} in (3a), there is a statistical dependence between z_{t+1} and u_{t+1} . In other words, since we allow for cross-correlation between the process noises entering on u_{t+1} and z_{t+1} , respectively, knowledge about u_{t+1} will contain information about z_{t+1} . This has to be taken into account when computing the second factor of the integrand in (28). To handle this, we make

use of a Gram-Schmidt orthogonalization to decorrelate the process noises. Let $\bar{v}_t^z = \bar{Q}_t^z v_t$, where

$$\bar{Q}_t^z \triangleq I - G_t^\top Q_t^{-1} G_t. \quad (30)$$

Note that \bar{Q}_t^z is a projection matrix: $(\bar{Q}_t^z)^2 = \bar{Q}_t^z$. It follows that $\mathbb{E}[\bar{v}_t^z (G v_t)^\top] = 0$ and $\mathbb{E}[\bar{v}_t^z (\bar{v}_t^z)^\top] = \bar{Q}_t^z$. We can then rewrite the dynamical equation (3a) as,

$$u_{t+1} = g_t + B_t z_t + G_t v_t, \quad (31a)$$

$$z_{t+1} = \bar{f}_t + \bar{A}_t z_t + F_t \bar{v}_t^z, \quad (31b)$$

where

$$\bar{f}_t = \bar{f}_t(u_t, u_{t+1}) \triangleq f_t + F_t G_t^\top Q_t^{-1} (u_{t+1} - g_t), \quad (31c)$$

$$\bar{A}_t = \bar{A}_t(u_t) \triangleq A_t - F_t G_t^\top Q_t^{-1} B_t, \quad (31d)$$

and where the process noises entering on u_{t+1} and z_{t+1} are now independent. Hence, from (31b), we can write

$$p(z_{t+1} | z_t, u_t, u_{t+1}) = \mathcal{N}(z_{t+1}; \bar{f}_t + \bar{A}_t z_t, F_t \bar{Q}_t^z F_t^\top). \quad (32)$$

The integral in (28) can now be computed by applying Lemma 1 with $c = \bar{f}_t$, $A = \bar{A}_t$, $x = z_t$, $\Gamma = F_t \bar{Q}_t^z$, $\Omega = \hat{\Omega}_{t+1}$ and $\lambda = \hat{\lambda}_{t+1}$. Combining this result with (29) and collecting the terms, we see that (28) coincides with (17) with,

$$Z_t = |Q_t|^{-1/2} |M_t|^{-1/2} \exp\left(-\frac{1}{2} \tau_t\right), \quad (33a)$$

$$\Omega_t = \bar{A}_t^\top \left(I - \hat{\Omega}_{t+1} F_t \Psi_t F_t^\top \right) \hat{\Omega}_{t+1} \bar{A}_t + B_t^\top Q_t^{-1} B_t, \quad (33b)$$

$$\lambda_t = \bar{A}_t^\top \left(I - \hat{\Omega}_{t+1} F_t \Psi_t F_t^\top \right) m_t, \quad (33c)$$

where we have defined the quantities

$$\tau_t = \|u_{t+1} - g_t\|_{Q_t^{-1}}^2 + \|\bar{f}_t\|_{\hat{\Omega}_{t+1}}^2 - 2\hat{\lambda}_{t+1}^\top \bar{f}_t - \|F_t^\top m\|_{\Psi_t}^2,$$

$$\Psi_t = \bar{Q}_t^z M_t^{-1} \bar{Q}_t^z,$$

$$M_t = \bar{Q}_t^z F_t^\top \hat{\Omega}_{t+1} F_t \bar{Q}_t^z + I,$$

$$m_t = \hat{\lambda}_{t+1} - \hat{\Omega}_{t+1} \bar{f}_t.$$

As opposed to the hierarchical model, the predicted backward statistics $\{Z_t, \Omega_t, \lambda_t\}$ all depend explicitly on u_t for this model. This implies that the backward prediction has to be done for each forward filter particle, see Algorithm 1. It should be noted, however, that the updating equations (33) can be simplified for some special cases of the mixed linear/nonlinear model (3). In particular, if the dynamics (3a) are Gaussian and linear in both z_t and u_t (the measurement equation (3b) may be nonlinear in u_t), it is enough to do one backward prediction. Models with linear dynamics and nonlinear measurement equations are indeed common in many applications, see [16].

4.4 Smoothing the linear states

Algorithm 1 provides a way of simulating nonlinear state trajectories, approximately distributed according to $p(u_{1:T} | y_{1:T})$. However, it is often the case that we are also interested in smoothed estimates of the linear states $\{z_t\}$. These estimates can be obtained by fusing the statistics from a forward conditional Kalman filter, with the backward statistics computed during the backward simulation. Note, however, that the forward statistics need to be computed anew; that is, we can *not* simply use the statistics from the forward RBPF. The reason is that the statistics should be computed conditionally on the nonlinear trajectories simulated in the backward sweep, which are in general different from the trajectories simulated by the RBPF.

Let $\tilde{u}_{1:T}$ be a backward trajectory generated by Algorithm 1. To compute the conditional smoothing PDF for z_t we start by noting that

$$p(z_t | \tilde{u}_{1:T}, y_{1:T}) \propto p(y_{t+1:T}, \tilde{u}_{t+1:T} | z_t, \tilde{u}_t) p(z_t | \tilde{u}_{1:t}, y_{1:t}). \quad (34)$$

Since the model is CLG, the latter factor can be computed by running a Kalman filter, conditionally on the fixed nonlinear state trajectory $\tilde{u}_{1:t}$. We get,

$$p(z_t | \tilde{u}_{1:t}, y_{1:t}) = \mathcal{N}(z_t; \tilde{z}_{t|t}, \tilde{P}_{t|t}), \quad (35)$$

for some mean vector $\tilde{z}_{t|t}$ and covariance matrix $\tilde{P}_{t|t}$, respectively (cf., (10)). By fusing this information with the backward information filter, given by (17), we get,

$$p(z_t | \tilde{u}_{1:T}, y_{1:T}) = \mathcal{N}(z_t; \tilde{z}_{t|T}, \tilde{P}_{t|T}), \quad (36a)$$

with

$$\tilde{z}_{t|T} = \tilde{P}_{t|T} \left(\tilde{P}_{t|t}^{-1} \tilde{z}_{t|t} + \lambda_t \right), \quad (36b)$$

$$\tilde{P}_{t|T} = \left(\tilde{P}_{t|t}^{-1} + \Omega_t \right)^{-1}. \quad (36c)$$

The resulting method can be seen as a forward-backward-forward smoother. First, a forward RBPF is used to filter the data. Second, a backward simulator is applied to simulate nonlinear state trajectories. Finally, a new forward sweep is carried out to compute the smoothing distributions for the linear states. The complete RBPS is given in Algorithm 2.

Similarly to above, we may also compute, for instance, the two-step smoothing distribution $p(z_{t-1:t} | \tilde{u}_{1:T}, y_{1:T})$ which is typically required when using the smoother for parameter estimation.

5 Extensions and computational aspects

5.1 Approximate Rao-Blackwellization

As pointed out in Section 1, an alternative to SMC is to use some deterministic Gaussian approximation of the filtering and smoothing distributions. This gives

Algorithm 2 Rao-Blackwellized particle smoother (RBPS)

1. **Forward filter/backward simulator:** Run Algorithm 1 to simulate a nonlinear state trajectory $\tilde{u}_{1:T}$. For each $t = 1, \dots, T$, store Ω_t and λ_t .
 2. **Linear state smoothing:**
 - (a) Run a Kalman filter for the linear states, conditionally on $\tilde{u}_{1:T}$. For each $t = 1, \dots, T$, store the filtered mean and covariance: $\{\tilde{z}_{t|t}, \tilde{P}_{t|t}\}$.
 - (b) Compute the smoothed means and covariances according to (36).
-

rise to methods such as the extended and the unscented Kalman filters and smoothers. In [31], an unscented two-filter smoother is constructed by inverting the dynamical model. However, as pointed out in [3], inversion of the dynamics will in general not lead to the correct result. Instead, [3] suggest a generalized two-filter smoothing formula and use this as a basis for an unscented two-filter smoother (see also [4]).

It is possible to combine these methods with the proposed RBPS. This enables smoothing for general nonlinear state-space models, in which one part of the state vector is approximated using particles and the other part of the state vector is handled using a deterministic approximation. This hybrid approach can be useful when deterministic approximations are found to be appropriate for some state variables, but insufficient for some other variables.

Consider the following, general nonlinear SSM,

$$x_{t+1} = \begin{pmatrix} u_{t+1} \\ z_{t+1} \end{pmatrix} = f(u_t, z_t, v_t), \quad (37a)$$

$$y_t = h(u_t, z_t, e_t). \quad (37b)$$

with process noise $v_t \sim \mathcal{N}(0, I_{n_v})$ and measurement noise $e_t \sim \mathcal{N}(0, I_{n_e})$, respectively. The partitioning of the state according to $x_t = (u_t, z_t)$ is in this case superficial, since the model is nonlinear in both variables. However, the partitioning is used to indicate which part of the model that we intend to address using particles, and which part that we intend to address using a deterministic approximation.

Approximate Rao-Blackwellized forward filtering can be done for the model (37) by using, for instance, an extended or an unscented RBPF [28]. These methods are based on different types of Gaussian approximations. Let $x \in \mathbb{R}^{n_x}$ be a Gaussian distributed random vector and let $\varphi : \mathbb{R}^{n_x} \rightarrow \mathbb{R}^{n_z}$ be some (nonlinear) transformation. A Gaussian approximation scheme can be used to find a Gaussian approximation of the random vector $z = \varphi(x)$. Examples of such approximations are first and second order Taylor expansions, i.e. linearizations, and the unscented transform [17]. Assume that the forward filter (10) holds approximately. We then seek a generalization of the backward information filter given by (17) and (18) to the nonlinear setting. We suggest an approach which

draws upon the generalized two-filter smoothing formula by [4, 3].

Consider first the backward prediction step (28). Let us introduce the auxiliary quantities

$$\gamma_t(z_t) \triangleq \mathcal{N}(z_t; \mu_t, \Sigma_t^z), \quad (38)$$

for some user-chosen parameters μ_t and Σ_t^z . In [4, 3], these functions are viewed as *artificial priors*. Indeed, if (38) is viewed as a prior distribution on z_t , then (37a) is a nonlinear transformation of the Gaussian vector (u_t is fixed),

$$\begin{pmatrix} z_t \\ v_t \end{pmatrix} \sim \mathcal{N} \left(\begin{pmatrix} \mu_t \\ 0 \end{pmatrix}, \begin{pmatrix} \Sigma_t^z & 0 \\ 0 & I_{n_v} \end{pmatrix} \right). \quad (39)$$

To exploit this, we write (28) as

$$\begin{aligned} & p(y_{t+1:T}, u_{t+1:T} | z_t, u_t) \\ &= \int p(y_{t+1:T}, u_{t+2:T} | z_{t+1}, u_{t+1}) \frac{\tilde{p}(x_{t+1}, z_t | u_t)}{\gamma_t(z_t)} dz_{t+1}. \end{aligned} \quad (40)$$

with $\tilde{p}(x_{t+1}, z_t | u_t) \triangleq p(z_{t+1}, u_{t+1} | z_t, u_t) \gamma_t(z_t)$. By using (39) and applying a Gaussian approximation scheme to the mapping,

$$\begin{pmatrix} x_{t+1} \\ z_t \end{pmatrix} = \begin{pmatrix} f(u_t, z_t, v_t) \\ z_t \end{pmatrix}, \quad (41)$$

we get

$$\begin{pmatrix} x_{t+1} \\ z_t \end{pmatrix} \stackrel{\text{approx.}}{\sim} \mathcal{N} \left(\begin{pmatrix} c_t \\ \mu_t \end{pmatrix}, \begin{pmatrix} \Sigma_t^x & \Sigma_t^{xz} \\ (\Sigma_t^{xz})^\top & \Sigma_t^z \end{pmatrix} \right), \quad (42)$$

for some vector c_t and matrices Σ_t^x and Σ_t^{xz} , respectively. Here, we have made the nonrestrictive assumption that the Gaussian approximation scheme applied to the identity mapping retains the Gaussian prior. By factorizing (42) we have

$$\tilde{p}(x_{t+1}, z_t | u_t) \approx \mathcal{N}(x_{t+1}; f_t^x + A_t^x z_t, Q_t^x) \gamma_t(z_t), \quad (43a)$$

where

$$A_t^x = \Sigma_t^{xz} (\Sigma_t^z)^{-1}, \quad (43b)$$

$$f_t^x = c_t - A_t^x \mu_t, \quad (43c)$$

$$Q_t^x = \Sigma_t^x - A_t^x (\Sigma_t^{xz})^\top. \quad (43d)$$

By plugging (43) into (40), we see that the factor $\gamma_t(z_t)$ cancels. We can thus use the approximate dynamics defined by (43) in the updating formulas for the backward prediction (33). To recover the notation used in (31) and (33), however, we need to split the quantities defined in (43) according to the two

state components u_{t+1} and z_{t+1} , respectively. That is, we define g_t , f_t , B_t , A_t , G_t and F_t through,

$$f_t^x = \begin{pmatrix} g_t \\ f_t \end{pmatrix}, \quad A_t^x = \begin{pmatrix} B_t \\ A_t \end{pmatrix}, \quad Q_t^x = \begin{pmatrix} G_t \\ F_t \end{pmatrix} \begin{pmatrix} G_t \\ F_t \end{pmatrix}^\top,$$

where the latter expression is given by for instance a Cholesky factorization of Q_t^x .

The backward measurement update (26) can be handled in a similar way. We write (26) as

$$p(y_{t:T}, u_{t+1:T} | z_t, u_t) = p(y_{t+1:T}, u_{t+1:T} | z_t, u_t) \frac{\tilde{p}(y_t, z_t | u_t)}{\gamma_t(z_t)}, \quad (44)$$

with $\tilde{p}(y_t, z_t | u_t) \triangleq p(y_t | z_t, u_t) \gamma_t(z_t)$ and $\gamma_t(z_t)$ being a user-chosen Gaussian density as in (38), possibly different from the one used in the prediction step. As above, with $\gamma_t(z_t)$ interpreted as an artificial prior, (37b) is a nonlinear transformation of the Gaussian vector,

$$\begin{pmatrix} z_t \\ e_t \end{pmatrix} \sim \mathcal{N} \left(\begin{pmatrix} \mu_t \\ 0 \end{pmatrix}, \begin{pmatrix} \Sigma_t^z & 0 \\ 0 & I_{n_e} \end{pmatrix} \right). \quad (45)$$

By applying a Gaussian approximation scheme to the mapping,

$$\begin{pmatrix} y_t \\ z_t \end{pmatrix} = \begin{pmatrix} h(u_t, z_t, e_t) \\ z_t \end{pmatrix}, \quad (46)$$

we get

$$\begin{pmatrix} y_t \\ z_t \end{pmatrix} \stackrel{\text{approx.}}{\sim} \mathcal{N} \left(\begin{pmatrix} d_t \\ \mu_t \end{pmatrix}, \begin{pmatrix} \Sigma_t^y & \Sigma_t^{yz} \\ (\Sigma_t^{yz})^\top & \Sigma_t^z \end{pmatrix} \right), \quad (47)$$

for some vector d_t and matrices Σ_t^y and Σ_t^{yz} , respectively. By factorizing (47) we have

$$\tilde{p}(y_t, z_t | u_t) \approx \mathcal{N}(y_t; h_t + C_t z_t, R_t) \gamma_t(z_t), \quad (48a)$$

where

$$C_t = \Sigma_t^{yz} (\Sigma_t^z)^{-1}, \quad (48b)$$

$$h_t = d_t - C_t \mu_t, \quad (48c)$$

$$R_t = \Sigma_t^y - C_t (\Sigma_t^{yz})^\top. \quad (48d)$$

The above quantities can then be used in the backward measurement update equations (27).

To apply the approximate RBPS as described above, we need to choose the artificial priors (38). In [4], it is suggested to use the actual ‘‘prior’’ $\gamma_t(z_t) = p(z_t | u_t)$ (recall that u_t is fixed at this stage of the algorithm), or some approximation of this density. However, it is also pointed out that the approach is more

generally applicable. Indeed, requiring $\gamma_t(z_t)$ to be close to $p(z_t | u_t)$ is only important if we want $\tilde{p}(x_{t+1}, z_t | u_t)$ and $\tilde{p}(y_t, z_t | u_t)$ to be close approximations to $p(x_{t+1}, z_t | u_t)$ and $p(y_t, z_t | u_t)$, respectively. For our purposes, this is not necessary, since the artificial priors cancel in (40) and (44). In fact, $\gamma_t(z_t)$ serves as a type of indicator for the operational range in the state-space of the Gaussian approximations. A more natural choice might thus be to use the current estimate of z_t to specify $\gamma_t(z_t)$, extracted either from the forward filter or from the backward filter. Indeed, if the Gaussian approximation scheme is based on a first order Taylor expansion, then the mean μ_t of the “artificial prior” is simply the linearization point for the Taylor expansion. It is easy to check that in this case (43b)–(43d) reduces to: $A_t^x = \frac{\partial f}{\partial z_t}(u_t, \mu_t, 0)$, $f_t^x = f(u_t, \mu_t, 0) - A_t^x \mu_t$, and $Q_t^x = \frac{\partial f}{\partial v_t}(u_t, \mu_t, 0) \frac{\partial f}{\partial v_t}(u_t, \mu_t, 0)^\top$. Hence, in this case the results will indeed be independent of the covariance matrix Σ_t^z of the artificial prior in (38), and choosing $\gamma_t(z_t)$ is equivalent to choosing the linearization point μ_t .

5.2 MCMC and particle rejuvenation

The FFBS algorithm [13] forms the basis for the proposed RBPS. It has been recognized that two shortcomings of this algorithm are: (i) its computational complexity is of order $O(NMT)$, which can sometimes be prohibitively large, and (ii) the states simulated in the backward pass are constrained to the support of the forward filter particles. However, in [5] a modification of FFBS which addresses both of these issues is proposed. The idea is to make use of Markov chain Monte Carlo (MCMC) within the backward simulator to generate the backward trajectories—the same technique can be used also with the proposed RBPS, as we discuss below.

As before, let $\tilde{u}_{t+1:T}$ be a partial backward trajectory. To extend this trajectory to time t , instead of simulating $u_{1:t}$ from the backward kernel approximation (14), we draw from some MCMC kernel which leaves the backward kernel invariant. Following [5], we use the RBPF particles, not from time t , but from time $t - 1$, to define the MCMC proposal:

$$q(u_{1:t} | \tilde{u}_{t+1:T}, y_{1:T}) \triangleq \sum_{i=1}^N \tilde{v}_{t-1}^i q(u_t | u_{1:t-1}^i, \tilde{u}_{t+1:T}, y_{1:T}) \delta_{u_{1:t-1}^i}(u_{1:t-1}),$$

where $\{\tilde{v}_{t-1}^i\}_{i=1}^N$ and $q(\cdot)$ are chosen by the user (see [5] for suggestions on how to select these quantities). Similarly to (13) we then factorize the target distribution as

$$\begin{aligned} p(u_{1:t} | u_{t+1:T}, y_{1:T}) &\propto p(y_{t+1:T}, u_{t+1:T} | u_{1:t}, y_{1:t}) \\ &\quad \times p(y_t | u_{1:t}, y_{1:t-1}) p(u_t | u_{1:t-1}, y_{1:t-1}) p(u_{1:t-1} | y_{1:t-1}). \end{aligned}$$

Using the RBPF particles at time $t-1$ to approximate this distribution we obtain

the Metropolis-Hastings acceptance probability for a proposed move $u_{1:t}^{(r)} \rightarrow u_{1:t}^*$,

$$\min \left\{ 1, \frac{\widehat{p}^N(u_{1:t}^* | \widetilde{u}_{t+1:T}, y_{1:T})}{q(u_{1:t}^* | \widetilde{u}_{t+1:T}, y_{1:T})} \frac{q(u_{1:t}^{(r)} | \widetilde{u}_{t+1:T}, y_{1:T})}{\widehat{p}^N(u_{1:t}^{(r)} | \widetilde{u}_{t+1:T}, y_{1:T})} \right\},$$

where

$$\begin{aligned} \frac{\widehat{p}^N(u_{1:t}^* | \widetilde{u}_{t+1:T}, y_{1:T})}{q(u_{1:t}^* | \widetilde{u}_{t+1:T}, y_{1:T})} &= \frac{w_{t-1}^* p(u_t^* | u_{1:t-1}^*, y_{1:t-1})}{\widetilde{v}_{t-1}^* q(u_t^* | u_{1:t-1}^*, \widetilde{u}_{t+1:T}, y_{1:T})} \\ &\quad \times p(y_{t+1:T}, \widetilde{u}_{t+1:T} | u_{1:t}^*, y_{1:t}) p(y_t | u_{1:t}^*, y_{1:t-1}) \end{aligned}$$

and analogously for the second factor (here, $\{u_{1:t-1}^*, w_{t-1}^*\}$ refers to the RBPF particle $\{u_{1:t-1}^i, w_{t-1}^i\}$ such that $u_{1:t}^* = (u_{1:t-1}^i, u_t^*)$).

Importantly, the expression above depends on the forward RBPF particle system only through the proposed sample $u_{1:t-1}^*$. Consequently, the computational complexity of simulating each individual backward trajectory is independent of the number of forward filter particles N . Hence, if we run the MCMC sampler for R steps at each time point we get a total computational complexity of order $O(RMT)$. As pointed out in [5], R can typically be chosen much smaller than N , resulting in a significant reduction in computational complexity. Furthermore, since we simulate u_t^* from (the possibly continuous) proposal density $q(\cdot)$, the backward trajectories are not constrained to the support of the forward filter particles.

A related technique is to use rejection sampling to simulate the backward trajectories, as has been proposed by [9] for the FFBS. However, this requires an upper bound on the backward sampling weights (15) that holds uniformly for all backward trajectories $\{\widetilde{u}_{t+1:T}^j\}_{j=1}^M$. It is not obvious how to choose this bound in the Rao-Blackwellized setting, making this technique less suitable for the RBPS.

5.3 Square-root implementation

As pointed out in Section 3.2, it is in general recommended to implement the conditional Kalman filter of the RBPF on square-root form, to ensure symmetry and positive definiteness of the involved covariance matrices. The same holds for the conditional backward information filter. In this section, we show how to implement the backward recursions given by (25), (27) and (33) on square-root form.

We use the technique proposed by [18], which is based on a numerically robust QR-factorization, and adapt this to the present setting. For an arbitrary matrix A , we can factorize it as $A = QR$, where Q is orthogonal and R is upper triangular. Let $\Omega_t^{1/2}$ be a matrix such that $\Omega_t = \Omega_t^{1/2} \Omega_t^{\top/2}$, and similarly for $\widehat{\Omega}_t$. Rather than computing the information matrices Ω_t and $\widehat{\Omega}_t$ in the backward filter, we will propagate the square-roots $\Omega_t^{1/2}$ and $\widehat{\Omega}_t^{1/2}$.

Consider first the backward measurement update (27). We compute a QR-factorization of the matrix,

$$\begin{pmatrix} \Omega_t^{\top/2} \\ (R_t^{1/2})^{-1}C_t \end{pmatrix} = \mathcal{Q} \begin{pmatrix} \mathcal{R}_1 \\ 0 \end{pmatrix}. \quad (49)$$

Here, $R_t^{1/2}$ can be computed by a Cholesky factorization of the measurement noise covariance matrix R_t . It follows that $\mathcal{R}_1^{\top}\mathcal{R}_1 = \Omega_t + C_t^{\top}R_t^{-1}C_t$, which implies that $\widehat{\Omega}_t^{1/2} = \mathcal{R}_1^{\top}$.

Next, we consider the backward prediction for the hierarchical CLG model, given by (25). We compute a QR-factorization of the following matrix:

$$\begin{pmatrix} I & 0 \\ \widehat{\Omega}_{t+1}^{\top/2}F_{t+1} & \widehat{\Omega}_{t+1}^{\top/2}A_{t+1} \end{pmatrix} = \mathcal{Q} \begin{pmatrix} \mathcal{R}_1 & \mathcal{R}_2 \\ 0 & \mathcal{R}_3 \end{pmatrix}. \quad (50)$$

It follows that

$$\begin{pmatrix} \mathcal{R}_1^{\top}\mathcal{R}_1 & \mathcal{R}_1^{\top}\mathcal{R}_2 \\ \mathcal{R}_2^{\top}\mathcal{R}_1 & \mathcal{R}_2^{\top}\mathcal{R}_2 + \mathcal{R}_3^{\top}\mathcal{R}_3 \end{pmatrix} = \begin{pmatrix} I + F_{t+1}^{\top}\widehat{\Omega}_{t+1}F_{t+1} & F_{t+1}^{\top}\widehat{\Omega}_{t+1}A_{t+1} \\ A_{t+1}^{\top}\widehat{\Omega}_{t+1}F_{t+1} & A_{t+1}^{\top}\widehat{\Omega}_{t+1}A_{t+1} \end{pmatrix}. \quad (51)$$

From (51) and (25), we can identify

$$\mathcal{R}_1^{\top}\mathcal{R}_1 = M_{t+1}, \quad (52a)$$

$$\mathcal{R}_2^{\top} = A_{t+1}^{\top}\widehat{\Omega}_{t+1}F_{t+1}M_{t+1}^{-1}\mathcal{R}_1^{\top}, \quad (52b)$$

$$\mathcal{R}_3^{\top}\mathcal{R}_3 = A_{t+1}^{\top}\widehat{\Omega}_{t+1}A_{t+1} - \mathcal{R}_2^{\top}\mathcal{R}_2 = \Omega_t. \quad (52c)$$

Hence, $\Omega_t^{1/2} = \mathcal{R}_3^{\top}$ and $\lambda_t = (A_{t+1}^{\top} - \mathcal{R}_2^{\top}\mathcal{R}_1^{-\top}F_{t+1}^{\top})m_{t+1}$.

Similarly, we can address the backward prediction for the mixed linear/nonlinear model (33) by computing the QR-factorization,

$$\begin{pmatrix} I & 0 \\ \widehat{\Omega}_{t+1}^{\top/2}F_t\bar{Q}_t^z & \widehat{\Omega}_{t+1}^{\top/2}\bar{A}_t \\ 0 & (Q_t^{1/2})^{-1}\bar{B}_t \end{pmatrix} = \mathcal{Q} \begin{pmatrix} \mathcal{R}_1 & \mathcal{R}_2 \\ 0 & \mathcal{R}_3 \\ 0 & 0 \end{pmatrix}. \quad (53)$$

By similar computations as above, we get $\Omega_t^{1/2} = \mathcal{R}_3^{\top}$ and $\lambda_t = (\bar{A}_t^{\top} - \mathcal{R}_2^{\top}\mathcal{R}_1^{-\top}\bar{Q}_t^zF_t^{\top})m_t$.

6 Experimental results

We evaluate the proposed RBPS on two numerical examples and compare its performance to alternative smoothers. The following methods are considered:

- FFBS: A non-Rao-Blackwellized FFBS [13].
- RB-KS: A Rao-Blackwellized Kitagawa smoother [20].
- RB-FF/JBS: Rao-Blackwellized forward filter/joint backward simulator [11].

- RB-FFBS: The proposed method (Algorithm 2).

For all methods, a bootstrap PF [14] or RBPF [7, 29] is used in the forward direction.

The RB-KS consists of running an RBPF and storing the nonlinear state trajectories. Smoothed linear state estimates are then computed by running constrained Rauch-Tung-Striebel (RTS) smoothers [26], conditionally on these nonlinear trajectories. The RB-FF/JBS is an adaptation of the “joint backward simulator” by [11], which runs an RBPF in the forward direction, but samples (u_t, z_t) jointly in the backward direction. The method relies on having access to the linear state samples in order to compute the backward sampling probabilities. In fact, the method given in [11] is only applicable to hierarchical CLG models, but we modify it to work also for mixed linear/nonlinear CLGs. Furthermore, we complement the method with constrained RTS smoothing to compute refined smoothed linear state estimates, which makes a more fair comparison (indeed, this is a simple “trick” that can be used to improve the performance of the method by [11]).

6.1 Estimation of a time-varying parameter

We consider first a 5th order mixed linear/nonlinear system. The nonlinear part is given by the time series,

$$u_{t+1} = 0.5u_t + \theta_t \frac{u_t}{1 + u_t^2} + 8 \cos(1.2t) + 0.071v_t^u, \quad (54a)$$

$$y_t = 0.05u_t^2 + e_t, \quad (54b)$$

for some process $\{\theta_t\}_{t \geq 1}$. The case with a static $\theta_t \equiv 25$ has been studied by, among others, [14]. Here, we assume instead that θ_t is a time varying parameter with known dynamics, given by the output from a 4th order linear system,

$$z_{t+1} = \begin{pmatrix} 3 & -1.691 & 0.849 & -0.3201 \\ 2 & 0 & 0 & 0 \\ 0 & 1 & 0 & 0 \\ 0 & 0 & 0.5 & 0 \end{pmatrix} z_t + 0.1v_t^z \quad (55a)$$

$$\theta_t = 25 + (0 \quad 0.04 \quad 0.044 \quad 0.008) z_t, \quad (55b)$$

with poles in $0.8 \pm 0.1i$ and $0.7 \pm 0.05i$. Combined, (54) and (55) is a mixed linear/nonlinear system. The noises are assumed to be white, Gaussian and mutually independent; $v_t^u \sim \mathcal{N}(0, 1)$, $v_t^z \sim \mathcal{N}(0, I)$ and $e_t \sim \mathcal{N}(0, 0.1)$.

We generate 1000 batches of data from the system, each with $T = 100$ samples. We run the smoothers two times, first with $N = 300$ and then with $N = 30$ particles. The backward-simulation-based methods use $M = N/3$ backward trajectories, based on the recommendation to set $M \lesssim N$ [23]. Table 1 summarizes the results, in terms of the time averaged root-mean-squared errors (RMSE) for the nonlinear state u_t and for the time varying parameter θ_t (note that θ_t is a linear combination of the four linear states z_t). We emphasize that

the RMSE values are computed with respect to the “true trajectories”, and not with respect to the optimal smoother (which is intractable). That is, even the optimal smoother would have resulted in a non-zero RMSE, and this should be taken into account when interpreting the results reported in the table.

Table 1: RMSE values averaged over 1 000 runs

Smoother	$N = 300$		$N = 30$	
	u_t	θ_t	u_t	θ_t
FFBS	0.499	0.782	1.203	1.238
RB-KS	0.424	0.660	0.980	0.909
RB-FF/JBS	0.399	0.579	0.967	0.869
RB-FFBS	0.398	0.564	0.965	0.836

The proposed RB-FFBS gives the most accurate results among the considered smoothers, both for $N = 300$ and $N = 30$. The difference between RB-FFBS and RB-FF/JBS is quite small. However, standard statistical hypothesis tests indicate indeed a clear statistically significant improvement for RB-FFBS over RB-FF/JBS. In fact, the small difference is not surprising, since these two methods are similar in many respects. We discuss this further in Section 7.

For further comparison, Figure 1 shows the estimates of θ_t for one specific batch of data, using $N = 300$ and $M = 100$. This reveals a clear difference between the methods’ abilities of accurately representing the posterior distribution of θ_t . For FFBS and RB-KS (the top row), there is a clear degeneracy in the trajectories. For RB-KS, this is expected, as it is a direct effect of the path degeneracy of the RBPF. For the (non-Rao-Blackwellized) FFBS, the degeneracy is caused by the fact that $N = 300$ particles is insufficient to represent the posterior in all five dimensions, resulting in that only a few particles get significantly non-zero weights. This will cause the backward simulator to degenerate, in the sense that many backward trajectories will coincide. The Rao-Blackwellized backward simulators (bottom row) perform much better in this respect, as there is a much larger diversity among the backward trajectories.

6.2 Tracking with a Constant Turn Model

Next we consider the task of tracking a manoeuvring target from noisy observations. A two dimensional constant turn model is used (see [21] for details). This has a single nonlinear state which describes the instantaneous turn rate of the target, and which evolves according to a random walk,

$$u_{t+1} = u_t + v_t^u. \quad (56)$$

The process noise v_t^u is modelled as Cauchy distributed centered at zero. The linear state vector comprises the position and velocity of the target in Cartesian

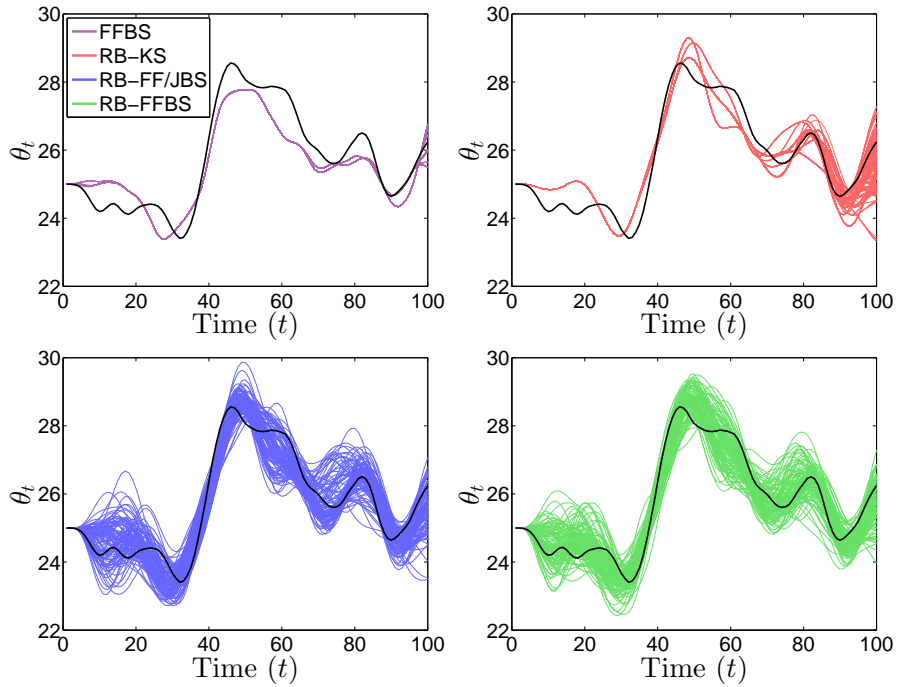


Figure 1: Estimates of θ_t for $t = 1, \dots, T$. From top left to bottom right; FFBS, RB-KS, RB-FF/JBS and RB-FFBS. Each curve corresponds to one particle trajectory ($\tilde{\theta}_{1:T}$ for FFBS and $\mathbb{E}[\theta_{1:T} | \tilde{u}_{1:T}, y_{1:T}]$ for the Rao-Blackwellized smoothers). The true value is shown as a thick black line.

coordinates. The transitions are described by the equation,

$$z_{t+1} = A(u_{t+1})z_t + F(u_{t+1})v_t^z, \quad (57)$$

with $v_t^z \sim \mathcal{N}(0, \sigma_z^2)$. See [21] for the definitions of $A(u_{t+1})$ and $F(u_{t+1})$. Noisy, radar-style observations are made of the target range and bearing from a fixed point (the origin),

$$y_t = \left[\tan^{-1} \left(\frac{z_{t,2}}{z_{t,1}} \right) \quad \sqrt{z_{t,1}^2 + z_{t,2}^2} \right]^\top + e_t, \quad (58)$$

where the observation noises in the bearing and range measurements are white, Gaussian and mutually independent, with variances σ_b^2 and σ_r^2 , respectively. This model cannot be Rao-Blackwellized directly, but may be treated using the approximate method of Section 5.1. Specifically, we use a linearization of the observation model (58) around the filter mean. That is, we set $\mu_t = z_{t|t}$ in (38) (as pointed out in Section 5.1, the resulting method is independent of the choice of covariance matrix Σ_t^z in (38) when using a first order Taylor expansion).

The algorithms were tested on one of the standard benchmark cases described in [2], with simulated observations made every second (see Figure 2). The spread of v_t^u is set to 0.03 rad/s, the process noise standard deviation $\sigma_z = 10$ m, and the observation noise standard deviations to $\sigma_b = \frac{\pi}{90}$ and $\sigma_r = 100$ m, respectively.

We simulated 100 batches of observations. The same four algorithms were tested as for the previous model. However, the non-Rao-Blackwellized particle filter regularly failed to track the target with a reasonable number of particles, making the FFBS impractical. It was thus excluded from the results. The approximate RBPF used $N = 100$ particles and the smoothers were used to sample $M = 100$ state sequences.

RMSE values for the smoothed state estimates are shown in Table 2. Again, we emphasize that the RMSE values are computed with respect to the true trajectory (Figure 2), and not with respect to the (intractable) optimal smoother. We see that RB-FFBS gives the most accurate results. However, the real advantage of the forward-backward smoothing algorithms is the increased number of unique particles (shown varying over time in Figure 3), which leads to a better characterisation of the posterior density. We can quantify this improvement by calculating the estimated posterior density of the true state $p(z_t | y_{1:T})$ for each approximation. This is plotted in Figure 4 and clearly shows the superior performance of the forward-backward smoothing algorithms over RB-KS. Also in this respect, the RB-FFBS algorithm appears to perform slightly better than the RB-FF/JBS.

The experiment was repeated with different model parameters and numbers of particles. Qualitatively similar results were observed.

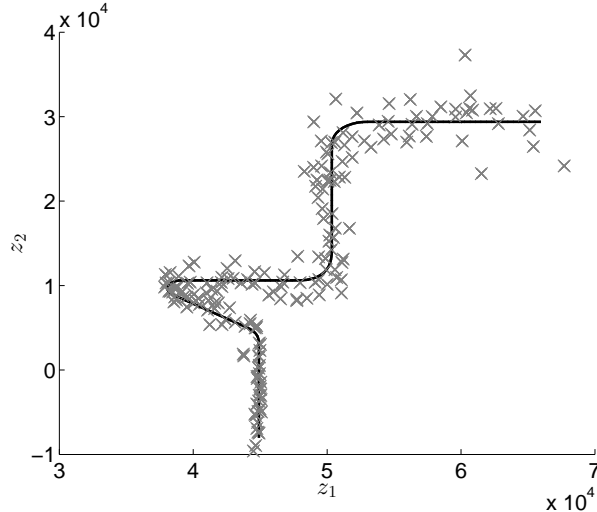


Figure 2: Benchmark fighter aeroplane trajectory from [2], with simulated observations (crosses).

Table 2: RMSE values averaged over 100 runs

Smoother	u_t	z_t
RB-KS	0.176	438
RB-FF/JBS	0.152	382
RB-FFBS	0.129	370

7 Discussion

We have derived, within a unified framework, an RBPS for two commonly encountered classes of conditionally linear Gaussian models; hierarchical CLG models and mixed linear/nonlinear CLG models, respectively. The method provides a solution to the offline (batch) state-inference problem. Furthermore, it can be combined with standard techniques, such as particle expectation maximization [6, 25] and particle MCMC [1] to address the system identification problem for these model classes (see [30] and [32] for these two approaches, respectively, applied to jump Markov systems). Compared to previously proposed RBPS, the proposed method differ on two key aspects: *(i)* it does not require any structural approximations of the model, and *(ii)* it Rao-Blackwellizes the linear state both in the forward direction and it the backward direction.

The second point is in contrast with the RB-FF/JBS [11], in which both the nonlinear and the linear states are simulated in the backward direction. Numerically, we found that the RB-FF/JBS performed quite similarly to the

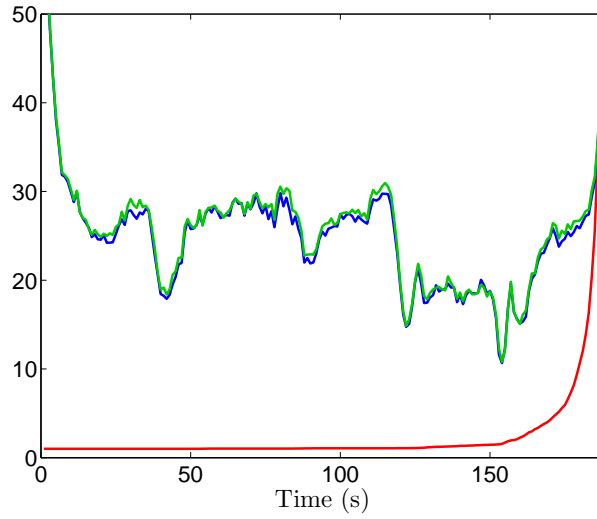


Figure 3: Average number of unique particles at each time step for RB-KS (red), RB-FF/JBS (blue), and RB-FFBS (green).

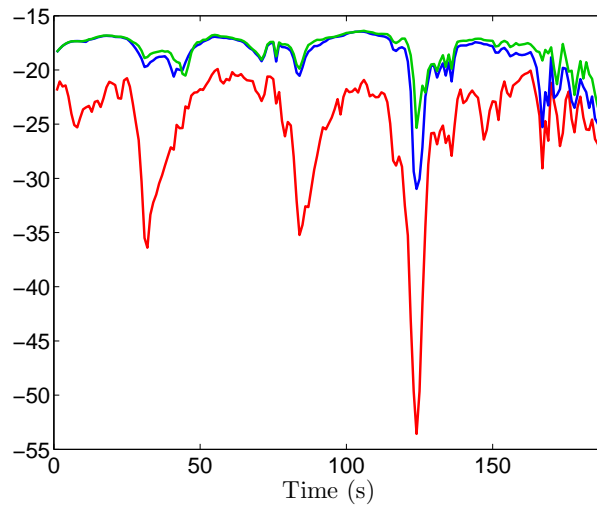


Figure 4: Average posterior log-density of the true state at each time step for RB-KS (red), RB-FF/JBS (blue), and RB-FFBS (green).

fully Rao-Blackwellized smoother (although, with a clear statistically significant difference in favour of the proposed method). This is not that surprising, since, essentially, the only difference between the methods is that for RB-FF/JBS the backward simulation weights are random (they depend on the linear state samples). This gives rise to unnecessary Monte Carlo variance which slightly deteriorates the performance of the method. In all other respects the two smoothers are very similar; in particular, they make use of the same forward RBPF to approximate the backward kernel. In terms of computational and implementation complexity they are almost identical. In fact, the RB-FF/JBS can be seen as an (unnecessary) approximation of the method proposed herein—this approximation makes the derivation, but not the implementation or execution of the algorithm, simpler. With this in mind we believe that the proposed RBPS indeed is the preferred method of choice of these two smoothers. Furthermore, in our opinion, the proposed method makes use of a more intuitively correct Rao-Blackwellization, since the marginalization is done both in the forward direction and in the backward direction.

References

- [1] C. Andrieu, A. Doucet, and R. Holenstein. Particle Markov chain Monte Carlo methods. *Journal of the Royal Statistical Society: Series B*, 72(3):269–342, 2010.
- [2] W D Blair, G A Watson, T Kirubarajan, and Y Bar-Shalom. Benchmark for radar allocation and tracking in ECM. *IEEE Transactions on Aerospace and Electronic Systems*, 34(4):1097–1114, 1998.
- [3] M. Briers. *Improved Monte Carlo Methods for State-Space Models*. PhD thesis, Department of Engineering, University of Cambridge, 2007.
- [4] M. Briers, A. Doucet, and S. Maskell. Smoothing algorithms for state-space models. *Annals of the Institute of Statistical Mathematics*, 62(1):61–89, February 2010.
- [5] P. Bunch and S. Godsill. Improved particle approximations to the joint smoothing distribution using Markov chain Monte Carlo. *IEEE Transactions on Signal Processing*, 61(4):956–963, 2013.
- [6] O. Cappé, E. Moulines, and T. Rydén. *Inference in Hidden Markov Models*. Springer, 2005.
- [7] R. Chen and J. S. Liu. Mixture Kalman filters. *Journal of the Royal Statistical Society: Series B*, 62(3):493–508, 2000.
- [8] N. Chopin. Central limit theorem for sequential Monte Carlo methods and its application to Bayesian inference. *The Annals of Statistics*, 32(6):2385–2411, 2004.

- [9] R. Douc, A. Garivier, E. Moulines, and J. Olsson. Sequential Monte Carlo smoothing for general state space hidden Markov models. *Annals of Applied Probability*, 21(6):2109–2145, 2011.
- [10] A. Doucet and A. Johansen. A tutorial on particle filtering and smoothing: Fifteen years later. In D. Crisan and B. Rozovskii, editors, *The Oxford Handbook of Nonlinear Filtering*. Oxford University Press, 2011.
- [11] W. Fong, S. J. Godsill, A. Doucet, and M. West. Monte Carlo smoothing with application to audio signal enhancement. *IEEE Transactions on Signal Processing*, 50(2):438–449, February 2002.
- [12] R. Gerlach, C. Carter, and R. Kohn. Efficient Bayesian inference for dynamic mixture models. *Journal of the American Statistical Association*, 95(451):819–828, 2000.
- [13] S. J. Godsill, A. Doucet, and M. West. Monte Carlo smoothing for nonlinear time series. *Journal of the American Statistical Association*, 99(465):156–168, March 2004.
- [14] N. J. Gordon, D. J. Salmond, and A. F. M. Smith. Novel approach to nonlinear/non-Gaussian Bayesian state estimation. *Radar and Signal Processing, IEE Proceedings F*, 140(2):107–113, April 1993.
- [15] F. Gustafsson. Particle filter theory and practice with positioning applications. *IEEE Aerospace and Electronic Systems Magazine*, 25(7):53–82, 2010.
- [16] F. Gustafsson, F. Gunnarsson, N. Bergman, U. Forssell, J. Jansson, R. Karlsson, and P.-J. Nordlund. Particle filters for positioning, navigation, and tracking. *IEEE Transactions on Signal Processing*, 50(2):425–437, 2002.
- [17] S. J. Julier and J. K. Uhlmann. Unscented filtering and nonlinear estimation. *Proceedings of the IEEE*, 92(3):401–422, 2004.
- [18] T. Kailath, A. H. Sayed, and B. Hassibi. *Linear Estimation*. Prentice Hall, Upper Saddle River, NJ, USA, 2000.
- [19] C.-J. Kim. Dynamic linear models with Markov-switching. *Journal of Econometrics*, 60:1–22, 1994.
- [20] G. Kitagawa. Monte Carlo filter and smoother for non-Gaussian nonlinear state space models. *Journal of Computational and Graphical Statistics*, 5(1):1–25, 1996.
- [21] X. R. Li and V. P. Jilkov. Survey of maneuvering target tracking. Part I: Dynamic models. *IEEE Transactions on Aerospace and Electronic Systems*, 39(4):1333–1364, 2003.

- [22] F. Lindsten, P. Bunch, S. J. Godsill, and T. B. Schön. Rao-Blackwellized particle smoothers for mixed linear/nonlinear state-space models. In *Proceedings of the 38th IEEE International Conference on Acoustics, Speech and Signal Processing (ICASSP)*, Vancouver, Canada, May 2013.
- [23] F. Lindsten and T. B. Schön. Backward simulation methods for Monte Carlo statistical inference. *Foundations and Trends in Machine Learning*, 6(1):1–143, 2013.
- [24] F. Lindsten, T. B. Schön, and J. Olsson. An explicit variance reduction expression for the Rao-Blackwellised particle filter. In *Proceedings of the 18th IFAC World Congress*, Milan, Italy, August 2011.
- [25] J. Olsson, R. Douc, O. Cappé, and E. Moulines. Sequential Monte Carlo smoothing with application to parameter estimation in nonlinear state-space models. *Bernoulli*, 14(1):155–179, 2008.
- [26] H. E. Rauch, F. Tung, and C. T. Striebel. Maximum likelihood estimates of linear dynamic systems. *AIAA Journal*, 3(8):1445–1450, August 1965.
- [27] S. Särkkä, P. Bunch, and S. Godsill. A backward-simulation based Rao-Blackwellized particle smoother for conditionally linear Gaussian models. In *Proceedings of the 16th IFAC Symposium on System Identification (SYSID)*, Brussels, Belgium, July 2012.
- [28] S. Särkkä, A. Vehtari, and J. Lampinen. Rao-Blackwellized particle filter for multiple target tracking. *Information Fusion Journal*, 8(1):2–15, 2007.
- [29] T. Schön, F. Gustafsson, and P.-J. Nordlund. Marginalized particle filters for mixed linear/nonlinear state-space models. *IEEE Transactions on Signal Processing*, 53(7):2279–2289, July 2005.
- [30] A. Svensson, F. Lindsten, and T. B. Schön. Identification of jump Markov linear models using particle filters. In *Proceedings of the 53rd IEEE Conference on Decision and Control (CDC)*, Los Angeles, USA, December 2014.
- [31] E. A. Wan and R. van der Merwe. The unscented Kalman filter. In S. Haykin, editor, *Kalman Filtering and Neural Networks*. John Wiley & Sons, 2001.
- [32] N. Whiteley, C. Andrieu, and A. Doucet. Efficient Bayesian inference for switching state-space models using discrete particle Markov chain Monte Carlo methods. Technical report, Bristol Statistics Research Report 10:04, 2010.